Pergamon

0892-6875(99)00147-8

Minerals Engineering, Vol. 13, No. 1, pp. 25-36, 2000

0892-6875/00/$ - see front matter

OXYGEN TRANSFER IN AGITATED SILICA AND PYRITE SLURRIES

J.J. DERKSEN[§], K. BUIST[§], G. VAN WEERT[¶] and M.A. REUTER[¶]

§ Kramers Laboratorium, Applied Physics Department, Delft University of Technology, Prins Berhardlaan 6, 2628 BW Delft, The Netherlands. E-mail jos@klft.tn.tudelft.nl
¶ Faculty of Applied Earth Sciences, Delft University of Technology, Mijnbouwstraat 120, 2628 RX Delft, The Netherlands.
(Received 16 December 1998; accepted 7 September 1999)

ABSTRACT

Oxygen transfer measurements in agitated mineral slurries were carried out in a 67 l laboratory tank. Two impellers (a Rushton turbine and a Lightnin A315) and two types of solid particles (silica, d_{50}=13 μm, and pyrite, d_{50}=14 μm) were investigated. Next to the volumetric oxygen transfer rate k_La, local bubble sizes, the overall gas hold-up in the tank, and the power input were measured. The silica and pyrite slurries behaved remarkably different with respect to the oxygen transfer as a function of the solids fraction. The pyrite particles increase k_La, whereas silica impairs oxygen transfer. The bubble size measurements indicate that the increased k_La in pyrite slurries is related to an increased interfacial area in the tank.

Keywords
Agitation; bioleaching

INTRODUCTION

Bio oxidation is a commercial process option and an accepted technology for processing refractory gold concentrates as is reflected in Table 1. These plants apply the BIOX® technology with Sao Bento applying a combination of BIOX®/pressure oxidation to treat the refractory values and subsequent cyanidation-CIL of the product to recover the gold.

TABLE 1 Presently operating bio leaching plants, employing the BIOX® technology, Hackl and Jones (1997)

Plant	*Feed analysis*				*Design Capacity*
	% S	*% Fe*	*% As*	*g/t Au*	*(t concentrate/day)*
Fairview (SA) - 1986	20.0			100-144	40
Sao Bento (Brazil) - 1991	18.7			30	150
Wiluna (Aus) - 1993	24.0	24.0	10.0	80-90	115
Sansu (Ghana) - 1994	11.4	17.5	7.7	48-76	720

Bacterial leaching may proceed either directly or indirectly and the mechanism is still not fully established, Leduc and Ferroni (1994). Direct leaching requires physical contact between the bacteria and the mineral particle surface under aerobic conditions. This process of direct bio-oxidation can be described according to the following reaction:

$$MS + 2\ O_2 + \text{bacteria} \rightarrow MSO_4 \text{ (where MS is the metal sulfide)} \quad (1)$$

For arsenopyrite this can be written as

$$FeAsS + 3.5O_2 + 2.5\ H_2O \rightarrow 0.5\ Fe_2O_3 + H_2SO_4 + H_3AsO_4 \quad (2)$$

During indirect leaching, the bacteria produces an oxidant which chemically oxidizes the sulfidic ore under acidic conditions (pH<2). *Thiobacillus ferrooxidans*, for example, generates and regenerates the oxidant (Fe^{3+}) which carries electrons from the mineral to the bacterium's cell membrane. These electrons are subsequently transported via an electron transport chain to molecular oxygen. The indirect leaching of pyrite is carried out via a series of chemical and bacterial reactions as presented by Eqs. 3 to 6.

$$2\ FeS_2 + 7\ O_2 + 2\ H_2O \rightarrow 2\ FeSO_4 + 2\ H_2SO_4 \quad (3)$$

$$4\ FeSO_4 + O_2 + 2\ H_2SO_4 + \text{bacteria} \rightarrow 2\ Fe_2(SO_4)_3 + 2\ H_2O \quad (4)$$

$$FeS_2 + Fe_2(SO_4)_3 \rightarrow 3\ FeSO_4 + 2\ S \quad (5)$$

$$S + 3\ O_2 + 2\ H_2O + \text{bacteria} \rightarrow 2\ H_2SO_4 \quad (6)$$

Therefore, when pyrite is exposed to air and water, a relatively slow chemical oxidation occurs that converts some of the pyrite into ferrous sulfate and sulfuric acid. If bacteria such as *Thiobacillus ferrooxidans* are present, a rapid oxidation of the ferrous sulfate occurs to produce ferric sulfate and water. It is understood that the ferrous iron acts as an electron donor for the bacterium. The ferric sulfate produced acts upon the pyrite to produce more ferrous sulfate and sulfur.

It is therefore evident from the above that since oxygen plays an important part in each reaction, oxygen transfer from the gas to the liquid phase is a crucial parameter in the design and operation of bio(oxidation) reactors. Apart from the oxidization of sulfide minerals, applications in the field of bioengineering (e.g. for environmental purposes, Buisman *et al.*, 1999) often encounter three-phase (gas–liquid–solid), stirred systems with oxygen transfer being a potential rate-limiting step.

In order to study the mass transfer in a slurry system, the oxygen transfer from air to mineral slurries in a Rushton turbine agitated tank was investigated using quartz particles with a mean diameter of 14μm in a tank of 67 l, Van Weert *et al.* (1995). This study did, however, not take the mass transfer in slurries containing sulfide minerals into consideration. It is the objective of this paper to discuss the mass transfer in pyrite slurries and compare the results to those obtained for a silica system. Precautions were taken to avoid oxidation of the pyrite; its role in these tests was as an inert slurry component. For comparison with the previous work, the tests were performed in the 67 l tank as well. Two impellers, viz. Lightnin A315 and Rushton, were used to compare their respective effects.

EXPERIMENTAL

The experimental setup is shown in Figure 1. The slurry is agitated in a flat-bottomed, 67 l vessel with four baffles at 90°. The (standard) dimensions of the tank, as well as of the two turbines used in the work presented are given in Figure 2. For this experimental setup the power input, the volumetric mass transfer coefficient (k_La), the overall gas hold-up, and (locally) the bubble size were measured as a function of the impeller speed, the solids fraction, and the gas flow rate. Two different types of impellers were investigated (see Figure 2): a Rushton turbine, and an axially pumping Lightnin A315; and two solids: silica and pyrite. An overview of the experimental conditions is given in Table 2.

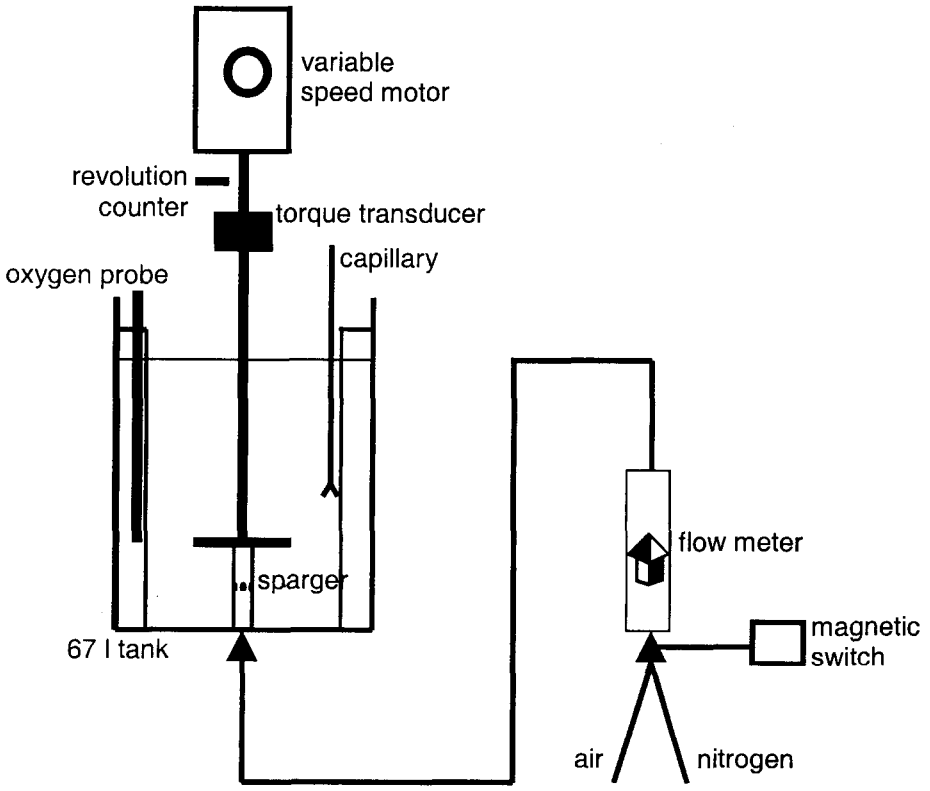

Fig.1 Overview of the experimental setup.

TABLE 2 Values of solids volume fractions, impeller speeds and gas flow rates (the superficial gas velocity is defined as the gas flow rate over the cross sectional area of the tank)

Rushton		*A315 Lightning*		*impeller speed [rpm]*	*gas flow [m^3/s]*	*superficial gas velocity [m/s]*
silica [vol%]	pyrite [vol%]	silica [vol%]	pyrite [vol%]			
0	1	0	1	500	$0.5 \cdot 10^{-3}$	$0.33 \cdot 10^{-2}$
5	3	5	3	550	$1.0 \cdot 10^{-3}$	$0.66 \cdot 10^{-2}$
10	5	10	5	600	$1.5 \cdot 10^{-3}$	$0.99 \cdot 10^{-2}$
30	10	15	10	650	$2.0 \cdot 10^{-3}$	$1.32 \cdot 10^{-2}$
	12.7		12.7	700		

Measurement techniques

The power input through stirring can be determined by measuring the impeller speed, and the torque exerted by the motor on the impeller shaft. The former is measured very accurately (within 0.1% error) by means of an optical sensor, attached to a counter. The torque is measured with a strain gauge system (Vibro-meter, type TT 106), responding to the shear stress in the shaft under torsion. The voltage signal was calibrated by determining the zero level, and the full scale voltage, which corresponds to 20 Nm. The torque is corrected for the no-fluid friction by subtracting the torque associated with the impeller revolving in air. The no-fluid friction was always less than 5% of the torque values measured in the slurries.

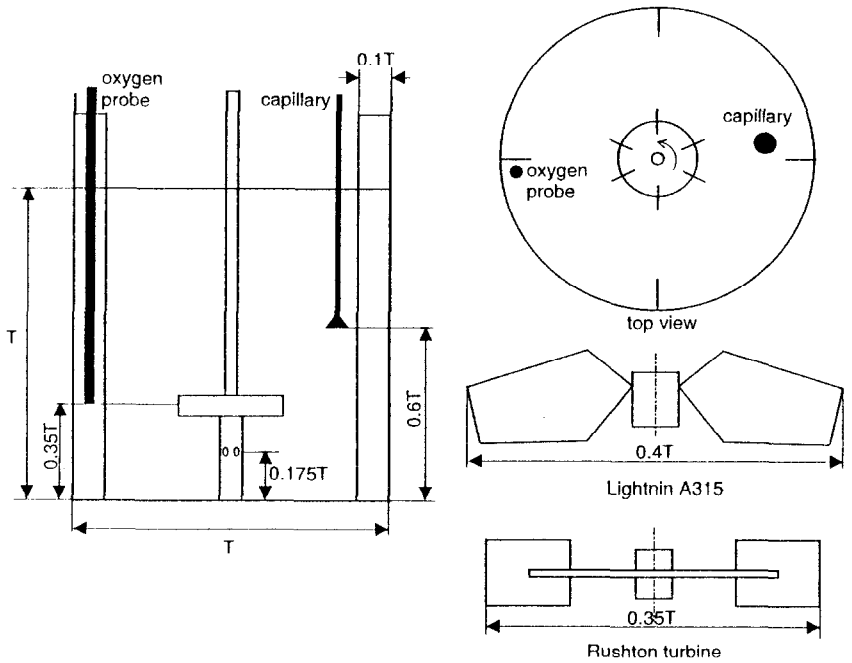

Fig.2 Dimensions of the tank, and the two impellers used in the present research. The positions of the oxygen probe, and of the capillary (for bubble size measurements) have been indicated as well. The tank diameter T=0.44 m.

The overall gas hold-up in the tank is determined by a visual inspection of the liquid level. Due to strongly turbulent fluctuations, the accuracy of this method is limited to approximately 10% of the hold-up value.

The so-called dynamic method for measuring k_La was adopted (Van Weert *et al.*, 1995; Mills *et al.*, 1987). In this method, the slurry is first deoxygenated by means of nitrogen. Subsequently the gas flow is suddenly switched to air. The response of the oxygen concentration in the slurry on this step-function in oxygen supply is recorded. In the ideal case of a very (infinitely) quickly responding oxygen probe, the response function to a switch of gas supply would be an exponential, with $-(k_La)\cdot t$ in the exponent (t denotes the time since switching to air). The oxygen probe, however, has a finite response time, mainly due to a mass transfer resistance in the Teflon membrane, which shields the electrolyte in the probe from the surroundings. The model used to describe the probe response reads

$$C_m = C_{eq}\left[1 - \frac{1}{k_La\cdot\tau - 1}\left(k_La\cdot\tau\cdot e^{-t/\tau} - e^{-k_La\cdot t}\right)\right] \tag{7}$$

with C_m the oxygen concentration measured by the probe, C_{eq} the equilibrium concentration, and τ the time constant of the probe. The latter was measured according to Dang *et al.* (1977). The procedure for determining k_La is to fit Eq. 7 to the measured probe response (see Figure 3). The non-linear fitting procedure has two independent fit parameters: k_La, and t_0. The latter is the origin of the time axis.

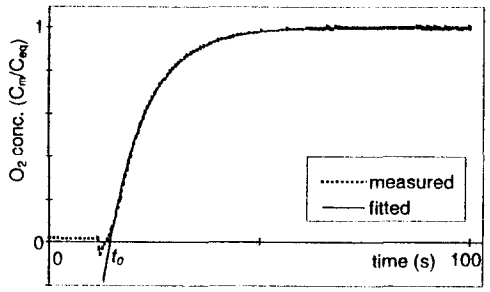

Fig. 3 Example of the fitting procedure in the dynamic method for determining k_La. Equation 7 (see text) was fitted to the measured curve.

Although the oxygen probe was placed in a quiet flow region, i.e. behind one of the baffles, the probe's membrane severely suffered from wear by the solid particles. Therefore, it had to be periodically replaced, leading to some variation in the time constant τ during the course of the experiments. From a sensitivity analysis, it could be concluded that a slight change in τ strongly affected the measured k_La value. For this reason, τ was determined on a regular basis. On average, the inaccuracy of k_La as a result of uncertainties in τ was estimated to be 4%. In the worst case (i.e. a high value of τ, combined with a high k_La) it could be as high as 8%.

In order to elucidate trends in bubble sizes during changing flow conditions, bubbles were measured at a single position in the tank (see Figure 2). The setup for the bubble size measurement consisted of a capillary with an internal diameter of 1.0 mm that sucked in bubbles, along with the slurry (Figure 4). The volume of the bubbles was probed with an optical system, based on light transmission through the capillary. The system (see Figure 4) measured the transit time (t_T) of a bubble, and the time delay (t_D) of the upper sensor signal with respect to the lower sensor. The bubble volume V can now be expressed in terms of t_T, t_D, d (the distance between both laser beams, see Figure 4), and the capillary diameter D:

$$V = \frac{\pi}{4} D^2 d \frac{t_T}{t_D} \tag{8}$$

The results on the bubble size measurements will be presented in terms of bubble diameters. This is the diameter d_B of a sphere with volume V. Typically 100 bubbles needed to be processed for a statistically converged value of the average bubble size.

It should be noted that the present method for probing bubbles has some possible bias sources. Obviously, due to turbulent flow conditions, the bubbles can not be extracted iso-kinetically. Therefore, bubbles can be torn apart (or coalesce) in the capillary. These effects have been minimized by placing the optical bubble probing system as close as possible (i.e. approximately 0.2 m) above the free surface in the tank, and by not allowing any bends in the capillary. Furthermore, the (finite) diameter of the capillary puts a bottom limit to the detectable bubble size. This bottom limit was estimated 1 mm, i.e. equal to the inner diameter of the capillary. It is believed that for the goal of the measurements, which is a qualitative observation on bubble sizes as a function of flow conditions, the present bubble probing method suffices.

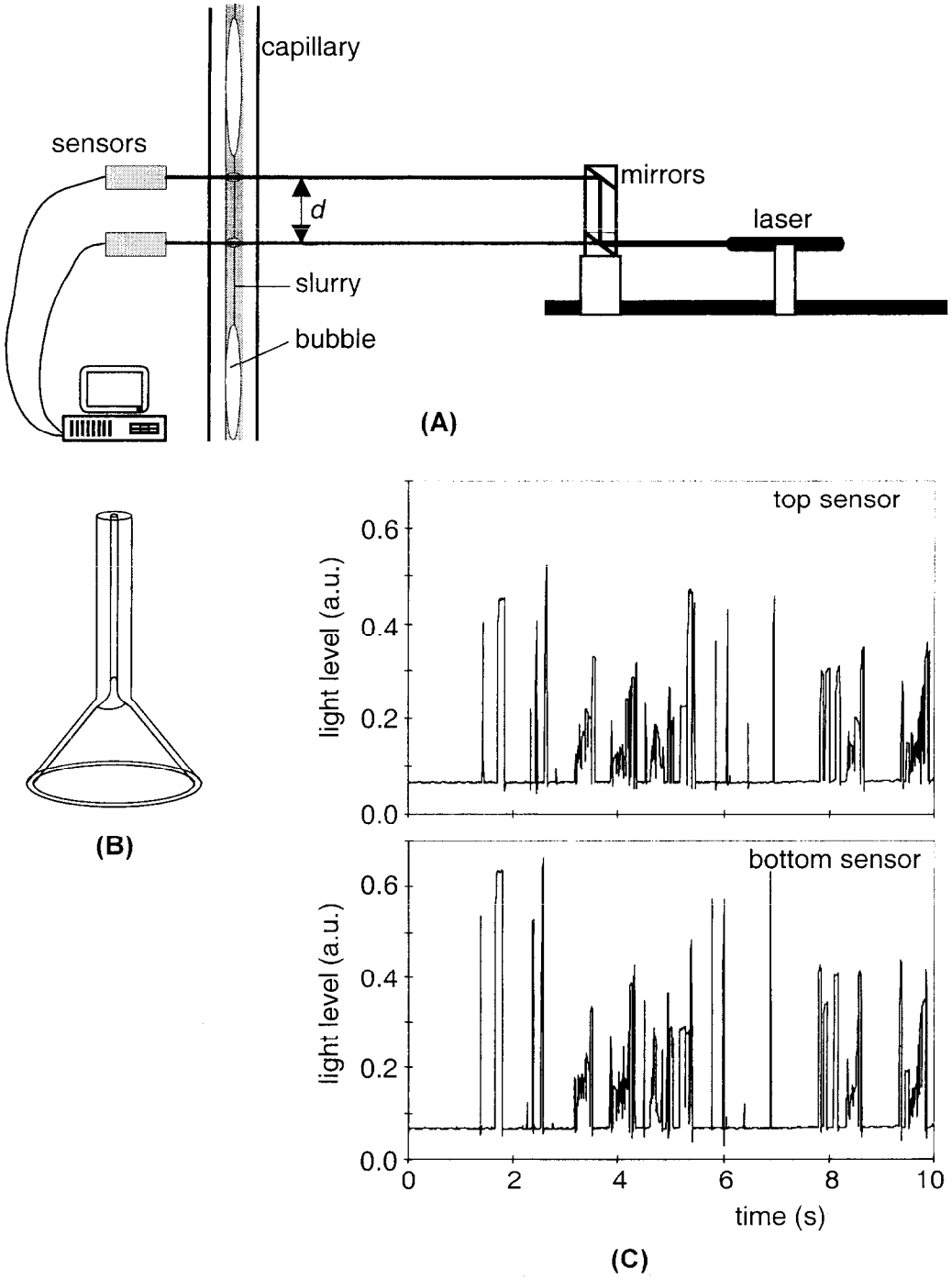

Fig.4 The setup for bubble size measurements. **(A)** Overview of the equipment. The distance d between the two laser beams amounted to 35 mm. **(B)** The conical head of the capillary. The internal diameter of the capillary was 1.0 mm. **(C)** Typical sensor signals. A high light intensity level denotes a bubble. Note the time shift between the two signals.

Solids

Two types of solids were used in the present study: silica and pyrite. The silica particles were from the same batch as used by Van Weert *et al.* (1995) (in their paper the particle size distribution was presented).

The mean diameter (d_{50}) was 13 μm, whereas 98% had a diameter less than 50 μm, the density was $2.61 \cdot 10^3$ kg/m^3. The pyrite was milled to irregularly shaped particles with a d_{50}=14 μm. The particle size distribution (see Figure 5) is markedly narrower than the distribution of silica. A d_{98}=35 μm can be deduced from Figure 5. The density of the pyrite was $5.0 \cdot 10^3$ kg/m^3. Please note that the slurry concentrations are reported as vol. %, not wt. %.

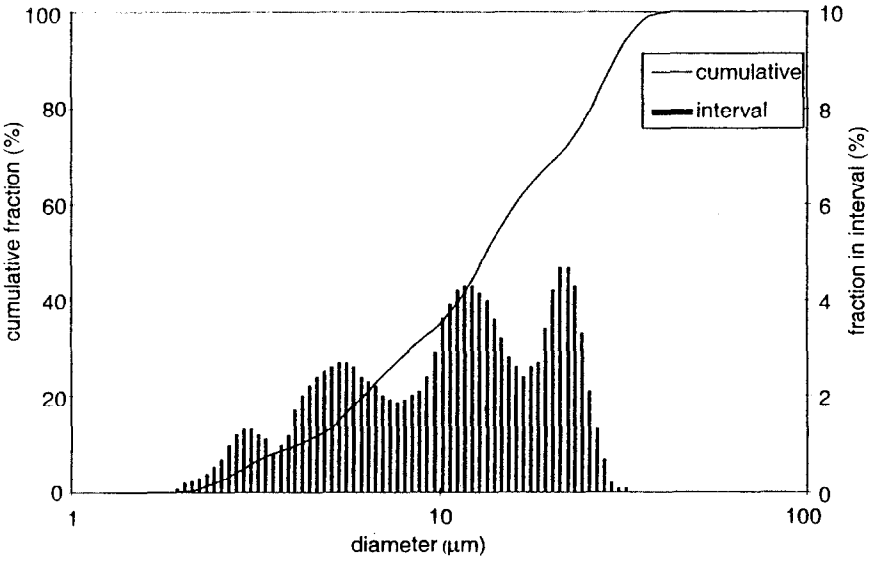

Fig. 5 Size distribution of the pyrite particles.

RESULTS

Volumetric mass transfer

First, the results of the k_La measurements will be discussed. In order to relate the present work with results presented in literature, the dependence of k_La on the gas flow rate will be discussed (see Figure 6). In the first place, it can be observed that the mass transfer coefficients in the pyrite slurries are much higher than in the silica slurries. Secondly, at the same flow conditions, in terms of impeller speed and gas flow rate, the Rushton turbine shows slightly higher k_La values, compared to the Lightnin A315 impeller. It should be noted, however, that the power inserted through stirring with the A315 is typically half the power needed to revolve the Rushton turbine at the same speed. In general, the A315 has an oxygen transfer rate (OTR), defined as the oxygen transfer (in kg) per unit stirring energy (kWh), typically 20 to 60% higher than the Rushton turbine.

In Figure 6, the present measurements are compared to a correlation on k_La published by Oguz *et al.* (1987). If we restrict ourselves to the dependence on the power input and the gas flow rate this correlation reads:

$$k_L a \propto P^{0.75} Q_{gas}{}^{0.5} \tag{9}$$

with P the power, and Q_{gas} the gas flow rate. The starting points of the lines in Figure 6 are the measurements at $Q_{gas}=0.5 \cdot 10^{-3}$ m^3/s. With the aid of Eq. 9, and the measured power input and gas flow rate, the mass transfer at the (three) higher gas flow rate levels can be predicted (see also Table 3). It can be concluded that the predictions provide a better result for the silica slurry, compared to the pyrite slurry. Current work is investigating surface properties, ionic strength, and specific density of the solids etc. as factors influencing these results.

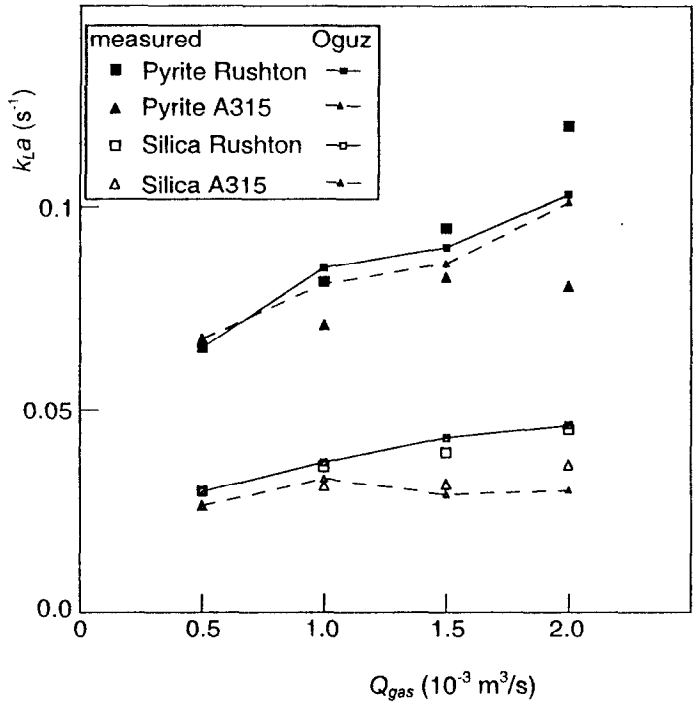

Fig.6 Volumetric mass transfer rate k_La as a function of the air flow rate. The solids fraction was 10 vol. % (for pyrite as well as for silica); the impeller speed was 500 rpm. The dots represent the present measurements; the lines represent values based on a correlation (see text) proposed by Oguz *et al.* (1987).

TABLE 3 Data as presented in Figure 6. The column k_La-Oguz was determined by means of Equation 9. At Q_{gas}=0.5·10^{-3} m^3/s, the *measured* k_La value was substituted in k_La-Oguz

Silica

Rushton				A315			
Q_{gas} [m^3/s]	P [kW/m^3]	k_La Oguz [s^{-1}]	k_La meas. [s^{-1}]	Q_{gas} [m^3/s]	P [kW/m^3]	k_La Oguz [s^{-1}]	k_La meas. [s^{-1}]
0.5·10^{-3}	2.48	0.0298	0.0298	0.5·10^{-3}	1.45	0.0262	0.0262
1.0·10^{-3}	2.07	0.037	0.0360	1.0·10^{-3}	1.27	0.033	0.0311
1.5·10^{-3}	1.94	0.043	0.0394	1.5·10^{-3}	0.80	0.029	0.0316
2.0·10^{-3}	1.77	0.046	0.0450	2.0·10^{-3}	0.70	0.030	0.0363

Pyrite

Rushton				A315			
Q_{gas} [m^3/s]	P [kW/m^3]	k_La Oguz [s^{-1}]	k_La meas. [s^{-1}]	Q_{gas} [m^3/s]	P [kW/m^3]	k_La Oguz [s^{-1}]	k_La meas. [s^{-1}]
0.5·10^{-3}	2.43	0.0652	0.0652	0.5·10^{-3}	1.67	0.0675	0.0675
1.0·10^{-3}	2.18	0.085	0.0814	1.0·10^{-3}	1.34	0.081	0.0709
1.5·10^{-3}	1.80	0.090	0.0948	1.5·10^{-3}	1.11	0.086	0.0852
2.0·10^{-3}	1.77	0.103	0.120	2.0·10^{-3}	1.14	0.101	0.0803

The effect of the solids on the volumetric mass transfer coefficient is strikingly different for silica and pyrite, see Figure 7. Compared to the no-solids case, the k_La values *increase* by typically 50% for a 12.7 vol.% pyrite slurry, whereas a *decrease* of about 40% is observed for a 15 vol.% silica slurry. Within the present range of parameters, the relation between solids volume fraction and k_La is approximately linear. The impeller speed and k_La are positively correlated: the higher the impeller speed, the higher k_La. The error

bars in Figure 7, however, indicate that especially at high k_La levels the differences in k_La at different impeller speeds are statistically not significant.

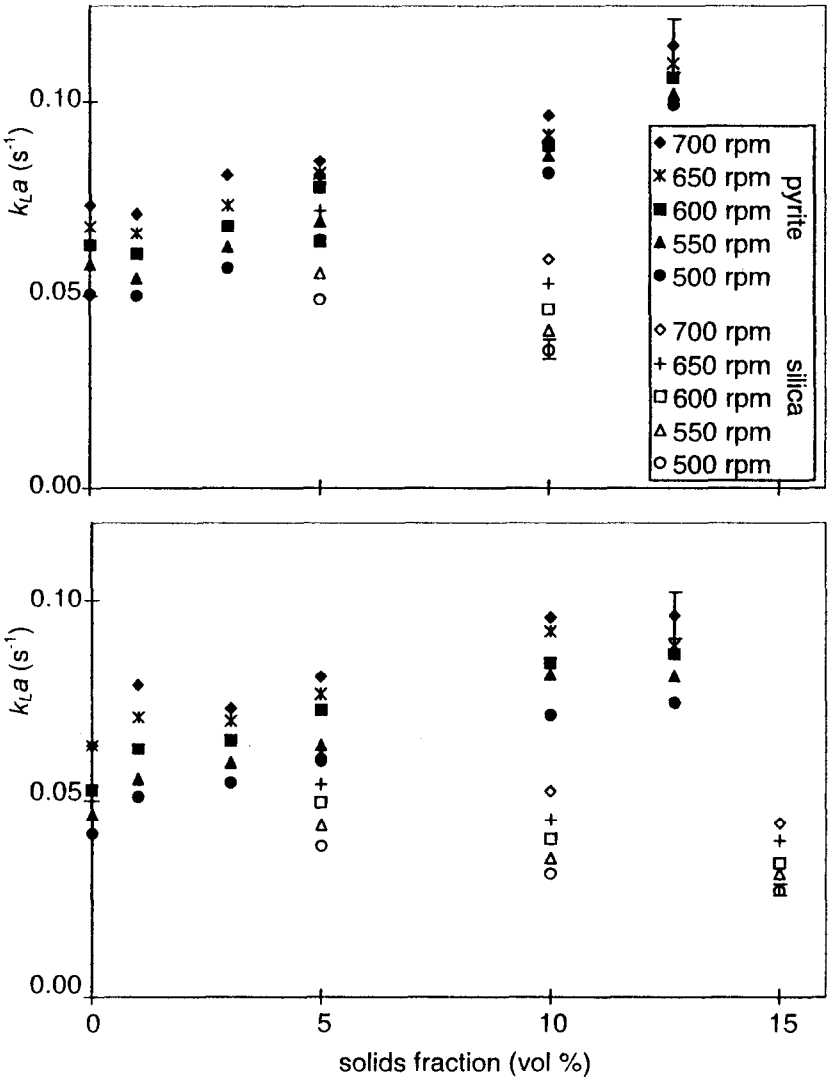

Fig.7 Volumetric mass transfer rate k_La as a function of the solids volume fraction at various impeller speeds, and at a gas flow rate of 1.0 l/s. Top figure: Rushton turbine; bottom figure: Lightnin A315. At the highest and lowest k_La value in each figure, an error bar has been drawn.

Bubble size and gas hold-up

The observations on k_La, made in the previous section, were the reason to separately investigate the specific interfacial area a. An appropriate way to measure a was not available. It would require local bubble size distribution and gas hold-up measurements. The measurement of the average bubble diameter, at a single location in the tank (see Figure 2), however, served as an indicator for the trends in the bubble size as a function of the flow conditions. Together with the (measured) overall gas hold-up, estimates on a could be obtained.

Results on all our bubble size measurements are presented (in a condensed manner) in Figure 8. In this figure, the individual flow conditions (defined by the impeller speed, gas flow rate, and solids fraction) are characterized by a single parameter viz. the power consumption. This leads to quite a scattered data set in terms of bubble sizes. Some coherent (albeit qualitative and very schematic) observations can, however, be

made. In the first place, the pyrite and silica slurries do *not* behave significantly different with respect to the bubble size. On average, the largest bubbles are found in case of a low (but not zero) volume fraction of solids. If the solids fraction is further increased, the size of the bubbles decreases. Only in the cases of the higher solids fractions, the data suggest enhanced bubble break-up (resulting in a smaller average bubble size) with increasing power.

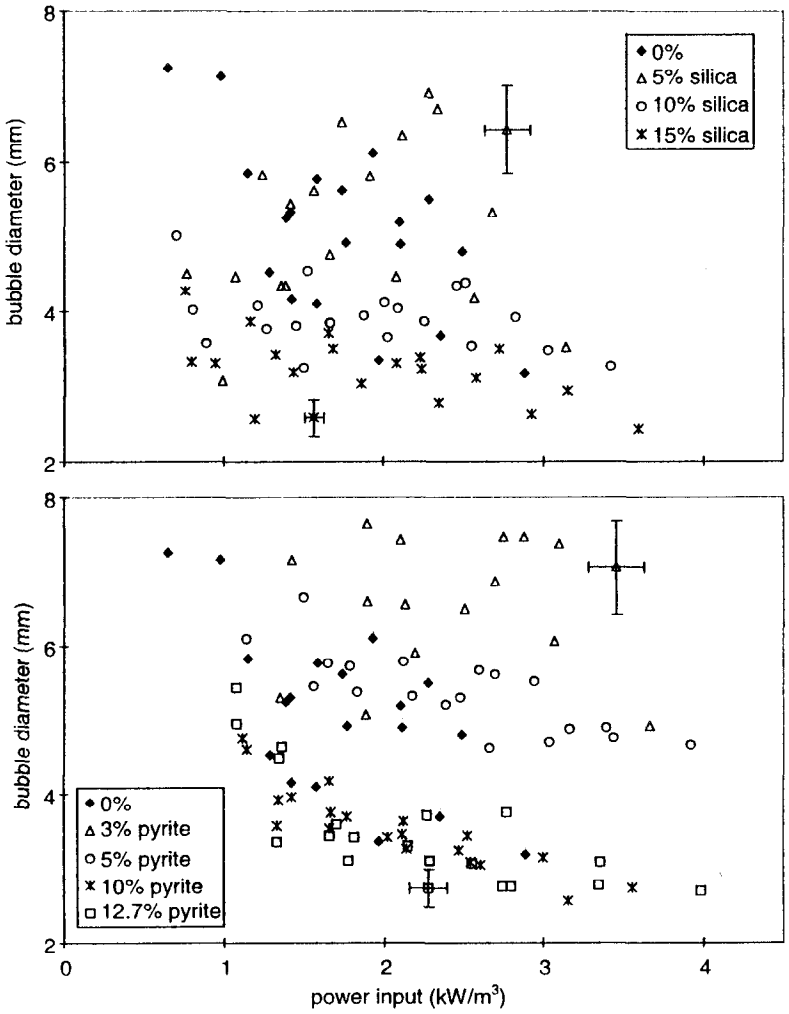

Fig. 8 The local bubble diameter (the measurement location has been indicated in Figure 2) as a function of the power input at various solid fractions. In the graphs, only a distinction is made with respect to the solids fraction, not with respect to impeller speed and gas flow rate. The latter parameters are contained in the specific power. Only data for the Lightnin A315 are shown. Error bars indicate the accuracy.

The overall gas hold-up reacts differently on the type, and the amount of solids in the slurry. For both impellers (i.e. Rushton and A315) an almost constant (or even slightly increasing) gas hold-up with increasing pyrite fraction was measured, whereas the gas hold-up significantly decreases (some 25% for the 15 vol.% solids) with increasing silica fraction (see Figure 9).

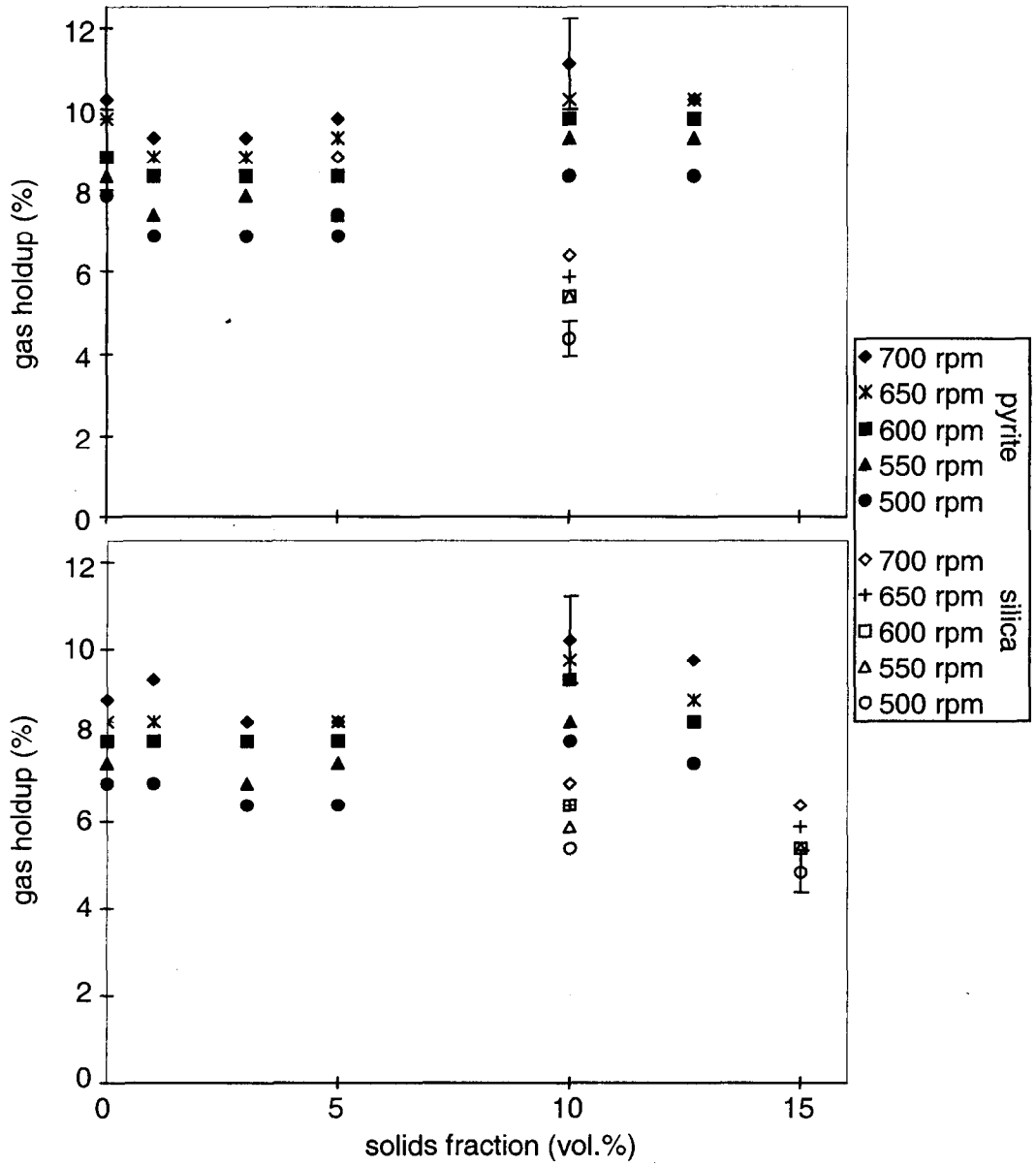

Fig.9 The gas hold-up as a function of the solids fraction at various impeller speeds, and at a gas flow rate of 1.0 l/s. Top graph: Rushton turbine; bottom graph Lightnin A315. Error bars indicate the accuracy

A tentative combination of the measured bubble diameter d_B (it has to be stressed again that this is a local, average value) and the overall gas hold-up α to a specific interfacial area a, according to

$$a = \frac{6\alpha}{d_B} \tag{10}$$

shows that in the silica slurries the interfacial area hardly depends on the solids fraction, in contrast to the pyrite slurries in which a increases significantly with increasing solids content.

DISCUSSION

Oxygen transfer in agitated slurries was investigated experimentally on a 67 l scale. The most remarkable effect observed was the different behavior of silica and pyrite slurries with respect to the oxygen transfer rate. When increasing the solids fraction, k_La increases in the pyrite system, whereas it decreases in case of silica. In conjunction with the k_La measurements, the overall gas hold-up and bubble sizes were measured. Although care should be taken when translating the locally collected bubble size data to overall parameters, these data seem to point at an increased interfacial area in pyrite slurries. At a constant mass transfer coefficient (k_L) level, the increased interfacial area might explain the enhanced k_La. Bubble size and gas hold-up measurements in the silica slurries indicate that the solids content hardly affects the interfacial area. The decreased k_La level might then be attributed to a lower k_L, possibly due to a blocking effect of (hydrophobic) silica at the gas–liquid interface.

In the presence of oxygen, the pH of the pyrite slurry will not remain constant, which was indeed measured in the pyrite slurry tests (after three minutes of stirring, the pH value of a 10% pyrite slurry dropped from 6.8 to 4.9). The effect of this changing chemical environment in the mixing vessel, thereby changing ionic strength, surface tension, surface properties of the mineral, and contact angle (hydrophobicity), has not been considered in this paper since pyrite oxidation was avoided as much as possible. In addition, parameters such as mineral density have also not been explicitly investigated. Current research is focusing on some of these parameters in order to understand the difference in the results between pyrite and silica slurries.

REFERENCES

Buisman, C.J.N., Vellinga, S.H.J., Janssen, G.H.R. and Dijkman, H., Biological sulfide production for metal recovery. *EPD Congress 1999*, Ed. B. Misra, TMS, Warrendale, 1999, pp 919–927.

Dang, N.P., Karrer, D.A. and Dunn, I.J., Oxygen transfer coefficients by dynamic model moment analysis. *Biotechnology and Bioengineering*, **19**, 1977, 853–864.

Hackl, R.P. and Jones, L., Bacterial sulphur oxidation pathways and their effects on the cyanidation characteristics of bio oxidised refractory gold concentrates. *IBS BIOMINE '97 Conference*, Sydney, 1997, pp M14.2.1–14.2.10.

Leduc, and Ferroni, G.D., The chemolithotrophic bacterium *Thiobacillus ferroxidans*. *FEMS Microbiology Reviews*, 1994, **14**, 103–116.

Mills, D.B., Bar, R. and Kirwan, D.J., Effect of solids on oxygen transfer in agitated three-phase systems. *AIChE Journal*, **33**, 1987, 1542–1549.

Oguz, H., Brehm, A. and Deckwer, W.D., Gas/liquid mass transfer in sparged agitated slurries. *Chemical Engineering Science*, **42**, 1987, 1815–1822.

Van Weert, G., Van der Werff, D. and Derksen, J.J., Transfer of O_2 from air to mineral slurries in a Rushton turbine agitated tank. *Minerals Engineering*, **8**, 1995, 1109–1124.

Correspondence on papers published in *Minerals Engineering* is invited, preferably by e-mail to bwills@min-eng.com, or by Fax to +44-(0)1326-318352